



**HAL**  
open science

## A new hybrid active-passive absorber with variable surface impedance

Benjamin Betgen, Marie-Annick Galland

► **To cite this version:**

Benjamin Betgen, Marie-Annick Galland. A new hybrid active-passive absorber with variable surface impedance. 10ème Congrès Français d'Acoustique, Apr 2010, Lyon, France. hal-00534632

**HAL Id: hal-00534632**

**<https://hal.science/hal-00534632v1>**

Submitted on 16 Nov 2010

**HAL** is a multi-disciplinary open access archive for the deposit and dissemination of scientific research documents, whether they are published or not. The documents may come from teaching and research institutions in France or abroad, or from public or private research centers.

L'archive ouverte pluridisciplinaire **HAL**, est destinée au dépôt et à la diffusion de documents scientifiques de niveau recherche, publiés ou non, émanant des établissements d'enseignement et de recherche français ou étrangers, des laboratoires publics ou privés.

# 10ème Congrès Français d'Acoustique

Lyon, 12-16 Avril 2010

## A new hybrid active-passive absorber with variable surface impedance

Benjamin Betgen, Marie-Annick Galland

Centre Acoustique du LMFA - UMR CNRS 5509 - Ecole Centrale de Lyon - 36, av. Guy de Collongue - 69134 Ecully Cedex, France

benjamin.betgen@ec-lyon.fr

Hybrid absorber are developed at the LMFA for about 10 years now. They are composed of distinct cells that each consist of a thin porous layer backed by a cavity. The latter contains an error microphone and a secondary source. Active control is used to reduce the acoustic pressure at the rear side of the porous layer at low frequencies. This results in a cancellation of the imaginary part of the surface impedance. (See also the paper “Caractérisation d’un absorbant hybride actif-passif par Vélométrie Laser Doppler”.) Choosing a porous layer with a resistance that equals the characteristic impedance of air, a normal incident plane wave (of arbitrary frequency) can be perfectly absorbed. In the case of grazing incidence, however, the optimal impedance (i.e. the one that produces the best absorption) is neither purely real nor constant with frequency. As a consequence, the choice of the porous layer represents a tradeoff between low and high frequency performance. A new type of hybrid absorber is therefore proposed. It contains one microphone on either side of the porous layer. In the presence of grazing flow, the front face microphone can be protected by a microperforated plate of high open area ratio. Normal velocity is simply estimated through the pressure gradient, which allows the determination of the surface impedance. This estimation is then subtracted from a target impedance to form a new error signal. The control system is realized as a digital feedback algorithm. Simulations and experiments show that typical optimal impedance functions for liners can be obtained. Measurements in a grazing incidence tube confirm that transmission loss can be significantly increased in respect to the former absorber.

## 1 Introduction

The context of the present study is the wall treatment of flow ducts. One important application for such wall treatments or liners are aero-engine nacelle inlets and outlets. In fact, previous experiments with a large number of hybrid cells mounted on a flow duct that opened out into an anechoic room approached this configuration to a certain extent [1].

This paper deals with a much simpler setup (i.e. one single hybrid cell in a tube with anechoic termination), but a more sophisticated control strategy (i.e. control of complex surface impedance).

The principle of the initial control strategy shall be recalled briefly: A hybrid cell is made of a resistive layer backed by a cavity. At low frequencies, the relation between acoustic pressure gradient and acoustic velocity through the thin layer can be approximated by the use of Darcy’s law. As a consequence, an estimation of the surface impedance is given by

$$Z = \frac{P_1}{V} = R \frac{P_1}{P_1 - P_2}, \quad (1)$$

with  $P_1$  the acoustic pressure at the front face of the resistive layer and  $P_2$  the one at the rear face. Cancellation of  $P_2$  obviously leads to the purely real and constant impedance of  $R$ , the resistance of the porous layer. Pressure cancellation is achieved by the use of a secondary source located on the rear side of the cavity. In the cited project, secondary sources were realized through piezoelectric patches. For simplicity, we use a

more bulky loudspeaker in the present study.

The active mode is limited to low frequencies, at higher frequencies the absorber acts as a classical  $\lambda/4$  resonator. The frequency separating both operation modes will be chosen somewhere below the resonance frequency of  $c/(4h)$ ,  $h$  being the cavity depth and  $c$  the speed of sound in air. One can therefore see the active mode as a way to cancel the (negative) imaginary part of the surface impedance that would otherwise be present at low frequencies. Choosing a porous layer with a resistance  $R$  that equals the characteristic impedance of air  $\rho c$ , a normal incident plane wave (of arbitrary frequency) can be perfectly absorbed. In the case of grazing incidence, however, the optimal impedance (i.e. the one that produces the best absorption) is neither purely real nor constant with frequency.

The new hybrid absorber has been developed with the objective to better approach optimal impedance.

## 2 Determination of optimal impedance

The value of the optimal impedance of a liner depends on many parameters like the geometry of the duct or flow parameters but also on how we define “optimal”. Maybe the most evident way is to define it as the impedance leading to maximum absorption. Cremer [2] found an analytic expression of this optimal impedance for a treatment of one face of an infinitely long rectangular duct. It is given as  $Z_{Cremer} = (0.91 - 0.76j) 2f h \rho$ ,

with  $h$  the side length of the duct perpendicular to the liner.

Tester [3] later found an expression that is almost identical to the one given by Cremer, but divided by  $(1 + M)^2$  to account for the presence of uniform flow of Mach number  $M$ .

For treatments of finite length, an alternative way to define optimal impedance is using the criterion of transmission loss (TL), i.e. both absorption and reflection contribute. A modal calculation has been performed in order to determine this optimal impedance for a liner of 6.6 cm x 6.6 cm size in a duct of 6.6 cm x 6.6 cm cross-section. In fact, this corresponds to our experimental facility MATISSE. The axial wave numbers inside the treated section are determined in a similar way as described in reference [4]. Propagation is supposed to follow an exponential pattern. Then, rigid sections upstream and downstream are connected to the treated section using continuity of pressure and velocity.

Results are plotted in figure (1) for the frequency range concerned by active control (lower frequencies can be controlled but the TL measurement is not optimized for frequencies below 500 Hz). For comparison, the modal calculation has also been performed for the “Cremer-case” and good agreement is found. We notice that optimal resistance for the finite case is lowered while optimal reactance remains almost unchanged. However, the global tendencies of the Cremer optimal impedance, i.e. a positive real part increasing with frequency and a negative, decreasing imaginary part, are retrieved. The following section deals with the development of an absorber intended to realize such surface impedances.

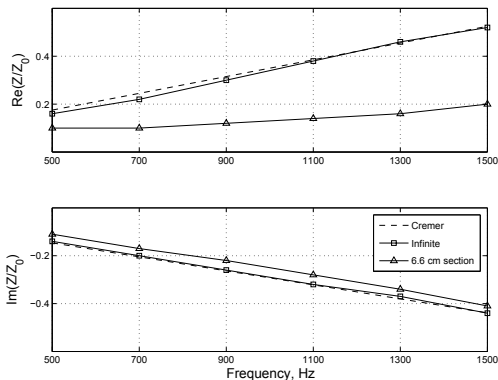


Figure 1: Optimal impedance for a liner of infinite length (Comparison Cremer formula/ modal calculation) and of 6.6 cm length (modal calculation) in a duct of 6.6 cm x 6.6 cm cross-section

### 3 Principle of the “complex” hybrid cell

Just as in the previous case, equation (1) is the basis for the new control strategy. The difference is that the target impedance  $Z_t$  is not the resistance  $R$  anymore but an arbitrary complex impedance. The error signal can then be written as follows:

$$E = Z_t(P_1 - P_2) - RP_1. \quad (2)$$

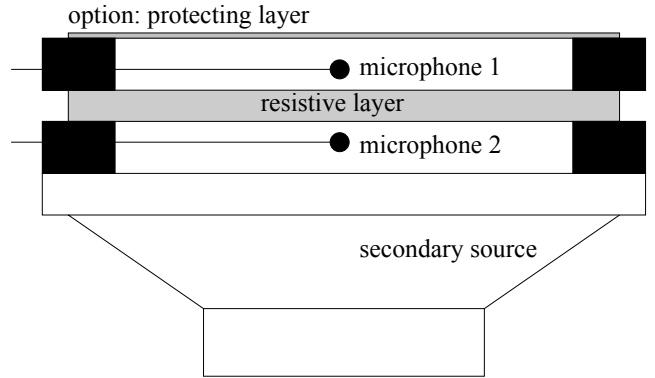


Figure 2: Scheme of the new hybrid cell

This method has initially been proposed by Dupont [5] for the realization of a purely imaginary impedance. A sketch of the corresponding hybrid cell is given in figure (2). The surface impedance is controlled at the position of the resistive layer. If an additional protecting layer is used, the surface impedance at the location of this layer is of course altered due to the added distance and the resistance of the layer. In this case, the target impedance has to be modified to compensate for this effect.

As impedance is implicitly defined in frequency domain,  $P_1$  and  $P_2$  in equation (2) are also defined in frequency domain. The microphone outputs are of course time domain signals, therefore the error signal has to be rewritten in time domain

$$\epsilon = H_z(p_1 - p_2) - Rp_1, \quad (3)$$

with a filter  $H_z$  representing the target impedance.

Considering the type of frequency response we seek (q.v. figure (1)), the identification of a stable and causal filter can be a difficult task. Typically, such filters feature amplitude responses that tend to infinity outside the targeted frequency band. We therefore propose an alternative way to realize complex target impedances in time domain. A real and constant target impedance  $Z_r$  for example doesn't pose any problem, as

$$E(\omega) = Z_r(P_1(\omega) - P_2(\omega)) - RP_1(\omega) \quad (4)$$

in frequency domain simply becomes

$$\epsilon(n) = Z_r(p_1(n) - p_2(n)) - Rp_1(n) \quad (5)$$

in (discrete) time-domain. Note that  $Z_r$  is a simple gain here. Let's now consider the realization of a purely imaginary impedance  $Z_i = i\alpha\omega$  which is proportional to frequency. With a negative proportionality factor  $\alpha$ , this represents the imaginary part of the Cremer/Tester impedance for instance.

$$E(\omega) = i\alpha\omega(P_1(\omega) - P_2(\omega)) - RP_1(\omega) \quad (6)$$

in frequency domain becomes

$$\epsilon(n) = \alpha(p_1'(n) - p_2'(n)) - Rp_1(n) \quad (7)$$

in time domain,  $p'$  designating the time derivative of  $p$ . So this type of impedance can be obtained using a derivator.

Combining real and imaginary part we obtain

$$\epsilon(n) = \alpha(p_1 - p_2)'(n) + Z_r(p_1(n) - p_2(n)) - Rp_1(n) \quad (8)$$

as an overall error signal for a target impedance with constant real part and (linearly) frequency dependent imaginary part. When the real part of the optimal impedance is almost constant (as in the presented example) this may be a useful compromise for broadband control. In the present study however, we focus on the control of time varying pure tones as the blade passing frequency of a fan. A digital feedback IMC-FxLMS architecture [6], well suited to his type of application, shall be used. The error signal of equation (8) is kept, but the resistance  $Z_r$  can now be a frequency dependent gain  $Z_r(\omega)$ .

## 4 Experimental setups

### 4.1 The hybrid absorber

Similarly to the “simple” hybrid cell, thin porous layers made of metal fibers such as wiremesh cloths or feltmetal sheets are suitable as resistive screens. In the present experiments, a wiremesh cloth glued on a perforated panel is used. The assembly represents a resistance of about  $0.5 \rho c$ . The surface of the cell measures  $6.6 \text{ cm} \times 6.6 \text{ cm}$ , the cavity is approximately  $2 \text{ cm}$  deep. As the rear side of the cavity is formed by a loudspeaker (Visaton SC 8 N) as secondary source, its depth is not completely homogeneous. Figure (3) shows the “complex” hybrid cell on the MATISSE tube. A Panasonic WM-64 electret condenser microphone is fixed on either side of the resistive screen. The front face layer is made of a microperforated panel with an open area ratio of 0.32 and  $0.54 \text{ mm}$  diameter perforations.

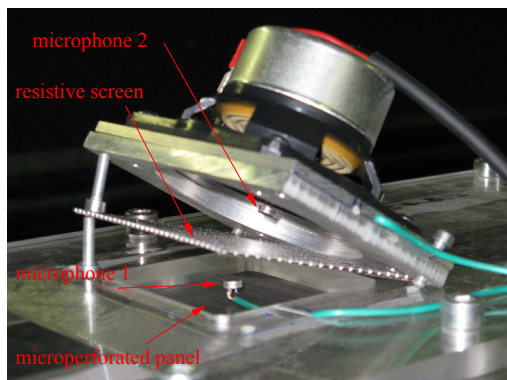


Figure 3: Picture of a hybrid cell mounted on the MATISSE tube

The IMC-FxLMS control scheme including the discussed error signal is built using SIMULINK® (Real Time Workshop) and executed on a dSpace® digital signal processor.

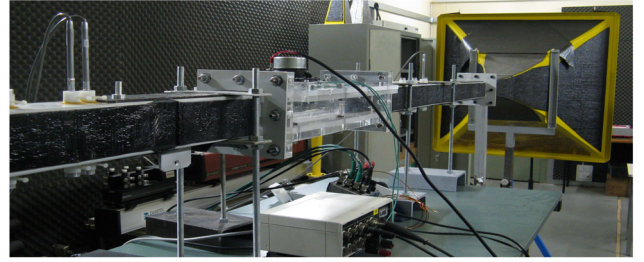


Figure 4: Picture of the MATISSE grazing incidence tube

### 4.2 The grazing incidence tube

The grazing incidence tube MATISSE is displayed in figure (4). It consists in a square cross-sectional duct ( $6.6 \text{ cm} \times 6.6 \text{ cm}$ ) whose length is approximately  $3.20 \text{ m}$ . The anechoic downstream termination is achieved thanks to an exponential outlet. The hybrid liner is applied on the upper wall of the test section. Three flush-mounted microphones (BK 1/4”), thereof two located upstream and one located downstream the test region, measure the differential pressure. The transfer functions between the primary source and the three microphones are recorded with a National Instruments® acquisition system. LabView® software is used to compute the Transmission Loss (TL). The studied frequency range from  $500 \text{ Hz}$  to  $1.5 \text{ kHz}$  remains in the plane-wave region.

### 4.3 The standing wave tube

The impedance realized by the hybrid cell is measured in a Kundt’s tube of cross-section  $5.5 \text{ cm} \times 5.5 \text{ cm}$  and  $1 \text{ m}$  length using the two-microphone method. The tube is designed for the test of active devices and equipped with a set of frames that permit to assemble a hybrid cell. Therefore, the cell tested in the standing wave tube is not exactly the same as the one that is used with the MATISSE tube. However, all critical distances are identical and the same passive layers and microphones are used.

## 5 Results

### 5.1 Impedance measurements

Impedance measurements have been performed using the described Kundt’s tube. Figures (5) and (6) show the realization of the Cremer impedance and the determined optimal impedance respectively. Note that the slope of the target reactance had to be increased to obtain the presented results. In fact, the porous layer is accounted for as a pure resistance, while in reality it also introduces a positive reactance, growing with frequency. As this error depends approximately linearly on frequency, it can be corrected for by (negatively) increasing the target reactance.

The presented target impedances are quite far from the characteristic impedance of air, absorption at normal incidence is therefore weak. As a consequence, resonances develop at certain frequencies and disturb the control signal.

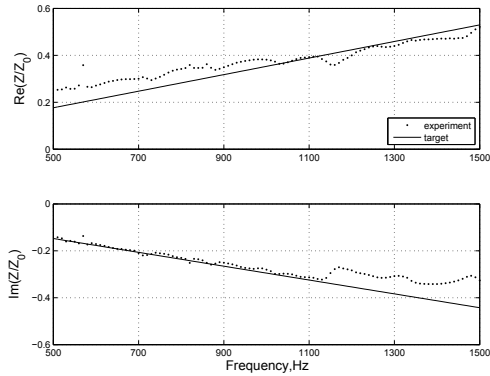


Figure 5: Experimental realization of the Cremer impedance

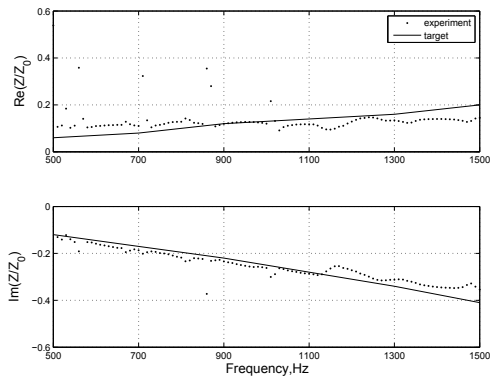


Figure 6: Experimental realization of the calculated optimal impedance

system (especially obvious in figure (6)). This problem does of course not occur in the grazing incidence tube.

## 5.2 Transmission Loss measurements

The Transmission Loss produced by one active cell as described in section 4.1 is measured using the grazing incidence tube MATISSE. Different control settings are compared in figure (7). The passive mode, resulting in very low TL in the considered frequency region is given as a reference. The simple active mode “ $p_2 = 0$ ” leads to an increase of TL, however, impedance control performs significantly better. As predicted, the calculated optimal impedance results in higher TL than the Cremer-impedance. However, slightly different settings, determined empirically, perform even better. As the realized impedances have been verified (Cf. previous section), the discrepancy between prediction and experiment might stem from the calculations. In fact, modal propagation inside the treated section is supposed to follow an exponential pattern. Even though the axial dependency of sound fields in ducts is often expressed that way, this is strictly speaking only correct in the case of infinitely long ducts.

Finally, the case of pressure cancellation on microphone one is given for comparison. The microperforated panel is of very low resistance, so this case is actually close to a pressure cancellation inside the duct. However, one observes that the corresponding TL decreases quickly with frequency (while the entire frequency

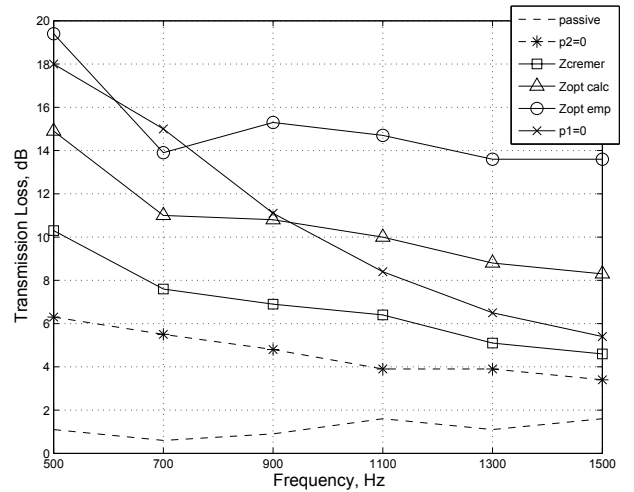


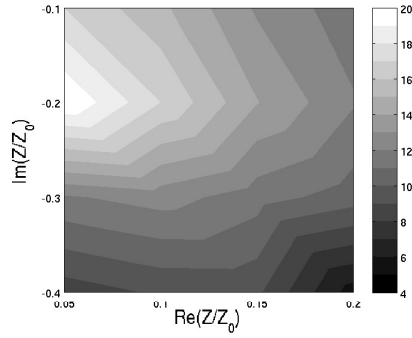
Figure 7: Transmission Loss realized with one hybrid cell

region remains well below the cut-off frequency of the duct!). This example serves as a proof that the active absorber works in a different way than classical “anti-noise“.

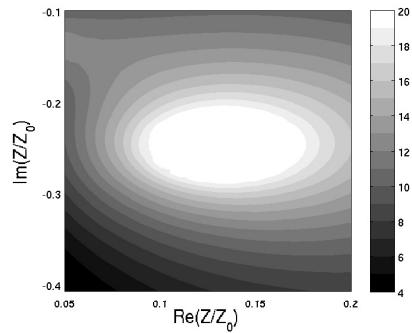
In order to experimentally determine the optimal impedance, the Transmission Loss over a grid of  $4 \times 4$  values in the complex impedance plane has been measured. Again, the tuning of each impedance has been checked using the standing-wave tube. The result is given in figure (8(a)). Figure (8(b)) displays the calculated TL. Obviously, optimal resistance and reactance are both lower than predicted, however, reactance is closer to the prediction. Figures (8(c)) and (8(d)) show the corresponding situation in the presence of a mean flow of Mach number 0.1. The difference now concerns rather the level of maximum TL than the position of the optimum. In fact, calculations predict a similar level, while the experiment reveals an important decrease of TL.

## 6 Conclusion

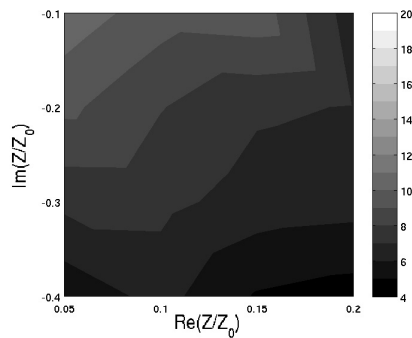
The developed impedance control concept has been shown suitable for the realization of typical optimal impedance functions for liners. Transmission Loss measurements revealed a significant increase of performance in respect to the former “ $p_2 = 0$ ” hybrid absorber. Values up to 20 dB have been measured with one single cell whose surface equals the cross-section of the flow duct. In the presence of flow of mean Mach number 0.1 in the direction of sound propagation, maximum Transmission Loss is reduced to about 10 dB. In the case of flow in the opposite direction, however, performance is likely to be less affected. At the moment, tuning of the absorber is quite complicated. On the one hand, there is a certain discrepancy between target impedance and measured impedance at higher frequencies. On the other hand, optimal impedance is often difficult to predict. An automatic sweep over the complex impedance plane and determination of the optimal settings would be an interesting option. Finally, multiple cells will have to



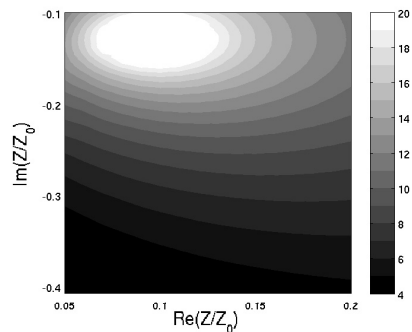
(a) Measured Transmission Loss,  $M=0$



(b) Calculated Transmission Loss,  $M=0$



(c) Measured Transmission Loss,  $M=0.1$



(d) Calculated Transmission Loss,  $M=0.1$

Figure 8: Comparison between measured and predicted Transmission Loss without and with grazing flow

be piloted simultaneously to obtain the desired "smart material". In the case of the simpler " $p_2 = 0$ " concept, this had been achieved thanks to a parallelized algorithm [6]. It will have to be shown if a similar algorithm is applicable to the new control strategy.

## Acknowledgments

This work has been supported by the French Ministerial Delegation for Armament (DGA) and the National Center for Scientific Research (CNRS).

## References

- [1] M.-A. Galland, B. Mazeaud, Design and testing of a hybrid passive/active acoustic treatment for nacelle inlets, *International Journal of Aeroacoustics* 6(1), pp. 45-59, 2007
- [2] L. Cremer, Theorie der Luftschall-Dämpfung im Rechteckkanal mit schluckender Wand und das sich dabei ergebende höchste Dämpfungsmaß, *Acustica* 3, pp. 249-263, 1953
- [3] B.J. Tester, The propagation and attenuation of sound in lined ducts containing uniform or "plug" flow, *Journal of Sound and Vibration* 28(2), pp. 151-203, 1973
- [4] S.W. Rienstra, A classification of duct modes based on surface waves, *Wave Motion* 37(2), pp. 119-135, 2003
- [5] J.-B. Dupont, Contrôle actif d'impédance acoustique pour la réduction de bruit transmis par un encoffrement, PhD Thesis, Ecole Centrale de Lyon, 2007
- [6] B. Mazeaud and M.-A. Galland, A multi-channel feedback algorithm for the development of active liners to reduce noise in flow duct applications, *Mechanical Systems and Signal Processing* 21(7), pp. 2880-2899, 2007